



This is a repository copy of *Noise suppression using local acceleration feedback control of an active absorber*.

White Rose Research Online URL for this paper:  
<http://eprints.whiterose.ac.uk/92441/>

Version: Accepted Version

---

**Article:**

Pelegrinis, M.T., Pope, S.A., Zazas, I. et al. (1 more author) (2015) Noise suppression using local acceleration feedback control of an active absorber. *Proceedings of the Institution of Mechanical Engineers, Part I: Journal of Systems and Control Engineering*, 229 (6). 495 - 505. ISSN 0959-6518

<https://doi.org/10.1177/0959651815573123>

---

**Reuse**

Unless indicated otherwise, fulltext items are protected by copyright with all rights reserved. The copyright exception in section 29 of the Copyright, Designs and Patents Act 1988 allows the making of a single copy solely for the purpose of non-commercial research or private study within the limits of fair dealing. The publisher or other rights-holder may allow further reproduction and re-use of this version - refer to the White Rose Research Online record for this item. Where records identify the publisher as the copyright holder, users can verify any specific terms of use on the publisher's website.

**Takedown**

If you consider content in White Rose Research Online to be in breach of UK law, please notify us by emailing [eprints@whiterose.ac.uk](mailto:eprints@whiterose.ac.uk) including the URL of the record and the reason for the withdrawal request.



[eprints@whiterose.ac.uk](mailto:eprints@whiterose.ac.uk)  
<https://eprints.whiterose.ac.uk/>

# Noise suppression using local acceleration feedback control of an active absorber

Michail T. Pelegrinis, Simon Pope, Ilias Zazas and Steve Daley

22nd December 2014

## **Abstract**

A popular approach for Active Noise Control (ANC) problems has been the use of the adaptive Filtered-X Least Mean Squares (FxLMS) algorithm. A fundamental problem with feedforward design is that it requires both reference and error sensors. In order to reduce the size, cost and physical complexity of the control system a feedback controller can be utilised. In contrast with FxLMS a feedback controller utilises local acceleration measurements of a sound-absorbing surface instead of global pressure measurements. Most control problems, including ANC, can be formulated in the General Control Configuration (GCC) architecture. This type of architecture allows for the systematic representation of the process and simplifies the design of a vast number of controllers that include  $H_\infty$  and  $H_2$  controllers. Such controllers are considered ideal candidates for ANC problems as they can combine near optimal performance with good robustness characteristics. This paper investigates the problem of reflected noise suppression in acoustic ducts and the possibilities and trade-offs of applying  $H_2$  control strategies. Hence, by

controlling locally the reflecting boundary structure, a global cancellation of the undesired noise can be accomplished. In the paper the  $H_2$  local feedback control strategy and performance are investigated using an experimental pulse tube. **The  $H_2$  design was chosen because it was able to provide consistently a stable response in contrast to the  $H_\infty$  design.**

## I Introduction

As an increased number of large industrial equipment such as engines, blowers, fans, transformers and compressors are in use, acoustic noise problems become more and more evident [1, 2]. Traditionally, the use of passive techniques has been the method of attenuating undesired acoustic sound waves with enclosures, barriers and silencers. The main problem that occurs when using passive control techniques is the limited efficiency at low frequencies therefore the use of active noise control (ANC) in order to reduce sound levels has been investigated thoroughly by the scientific community, particularly for acoustic ducts, and a large number of control schemes have been proposed [1]. Due to the fact that reflecting sound waves are a key contributor in acoustic resonances, this paper focuses on noise suppression through the reduction of the reflected sound wave in an experimental pulse tube, figure 1.

Classical ANC control procedures concerning cancellation of reflected noise often make use of distributed microphones and loudspeakers in order to generate appropriate signals for secondary sources. Such designs often use variants of the Filtered-X Least Mean Square (FxLMS) algorithm and examples can be found in the work of various authors [3, 4]. These control procedures, however, can lead to complex solutions to

implement and also generate significant measurement noise. In this paper a control scheme that is simple to implement and is focussed on using local measurements in contrast to the remote error microphone required in FxLMS designs is proposed. In order to achieve a reduction in the reflection of sound the approach here is to directly control the dynamics of the terminating boundary surface inside the acoustic duct.

Recent work in the field of ANC has been focused on designing actuator set-ups that will enable active structural acoustic control (ASAC) of low frequency noise radiated by vibrating structures [4]. The work described by these authors explores the development of thin panels that can be controlled electronically so as to provide surfaces with desired reflection coefficients. Such panels can be used as either perfect reflectors or absorbers. The development of the control system is based on the use of wave separation algorithms that separate incident sound from reflected sound. The reflected sound is then controlled to desired levels. The incident sound is used as an acoustic reference for feedforward control and has the important property of being isolated from the action of the control system speaker. The suggested control procedure makes use of a half-power FxLMS algorithm and therefore requires installation of microphones in order to be applicable and the use of low pass filters, which adds significant complexity to the solution of the primary problem.

Another approach in the field of ASAC which can reduce the inherent complexity of the previous approach is the application of a low frequency volume velocity vibration control procedure for a smart panel in order to reduce sound transmission [5]. The control algorithm makes use of a simple velocity feedback controller in order to add damping to the resonant frequencies of the controlled panel. The addition of damping will reduce the vibration that occurs when an incident acoustic wave impacts the panel

and will thereby reduce the acoustic radiation efficiency. A more refined control design approach in the field of ASAC is to implement a  $H_2$  multi-variable feedback control design [6]. In this work, an array of collocated piezoelectric sensor-actuators are utilised in order to reduce the total radiated sound power of a simply supported thin plate. The main problem when implementing this type of control is the fact that the thin plate used to suppress the noise is not an efficient sound generating device and therefore will have significant performance limitations (noise reduction).

Another approach found in the literature considers a  $H_\infty$  control strategy as part of a hybrid feedforward - feedback control design [7]. This approach combines the benefits of both previous mentioned designs (FxLMS and ASAC). The problem of this strategy is the high resource demand due to the feedforward controller. Furthermore, contrast to the ASAC design the  $H_\infty$  feedback design requires global measurements of the plant (error microphone signal) which increases the implementation complexity significantly.

Finally, an important application of ANC with the aim of developing ideal absorbers should be mentioned. Specifically, the work focuses on how to transform a loudspeaker in an active electroacoustic resonator [8]. With the aid of sensors (microphones, optical velocity sensor) and control system, the proposed control designs make use of simple lead lag velocity feedback controllers that are able to achieve broadband sound absorption at the transducer diaphragm. The disadvantage of this method is that it relies on empirical fine-tuning of the controller and therefore fails to address the ANC problems in a more general manner.

The aim of this research is to develop a generalised output feedback controller for an acoustic duct system as illustrated in figure 2. The control scheme will make use solely

of local measurements (acceleration) of the reflecting boundary surface (**loudspeaker**) in order to suppress the undesired reflecting sound waves that occur in the presence of an incident disturbance sound wave. **The proposed method is demonstrated using an acoustic duct apparatus.** However, due to the local nature of the design, it is possible to expand this control strategy for noise reduction of reflecting sound waves within large enclosures (i.e. representative of many industrial environments). The only difference to the implementation procedure would be the modelling of the acoustical environment. Hence given the plant's dynamics, the suggested method can be applied to a wide range of noise reduction problems such as one dimensional (ducts and with modified actuation, pipeline flow noise), large enclosures (transportation and industrial environments) and even free-field problems (highway noise barriers, for example). In order to appreciate the benefits the proposed feedback control design has to offer the popular FXLMS approach is also considered.

The paper is organised as follows: In Section II a description of the experimental acoustic duct system is provided. In Section III the **calibration and** separation technique utilised to retrieve the reflecting sound wave is presented. In Section IV the  $H_2$  output feedback control design approach, which is proposed to cancel the undesired reflecting sound wave is detailed. In Section V the popular FXLMS control design is detailed. In Section VI the formulation of the control loop and experimental results illustrating the two designs and comparison with regards to performance and implementation complexity is presented. Finally, Section VII provides some concluding remarks.

## II Experimental test rig

Figure 1 shows a photograph of the system that comprises the acoustic duct with the disturbance source, a secondary control source and the three sensors required to develop the control strategy. The set-up consists of two Visaton W 100 s loudspeakers; the first one is acts as a disturbance source and the second one is acts as the control source. The sensors required for the experiment are two Cirrus MV:181A pressure microphones in order to retrieve the pressure of the total standing sound wave and calculate the reflecting sound wave and an accelerometer (PCB 352A24 accelerometer) that will measure the acceleration of the control loudspeakers cone. It is important to state that the microphones are only present so as to monitor the performance of the proposed control design by modelling the plant's dynamics; only the accelerometer is required for control system implementation. Furthermore, the experimental rig comprises of an additional number of elements (dSPACE with PPC 1103 Controller Board, two Labworks PA-119 Power Amplifiers and a FYLDE 256AC Pre-amplifier), which can be viewed in the photos presented in figure 3.

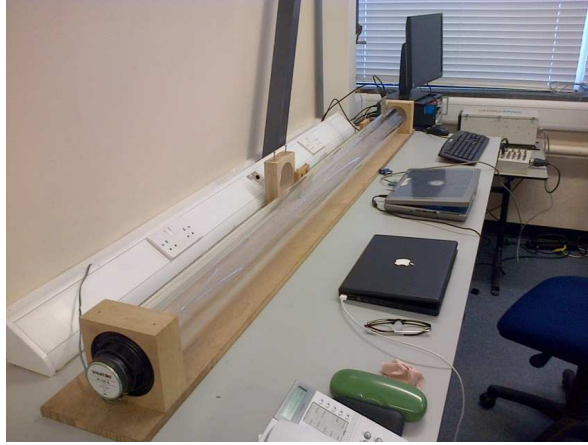


Figure 1: Picture of the experimental acoustic tube consisting of the disturbance source (near end), control source (far end) and the three sensors (two microphones and the accelerometer).

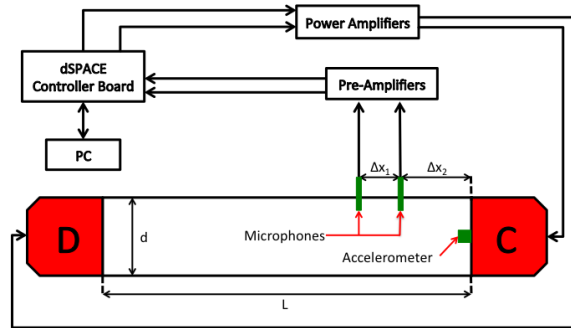
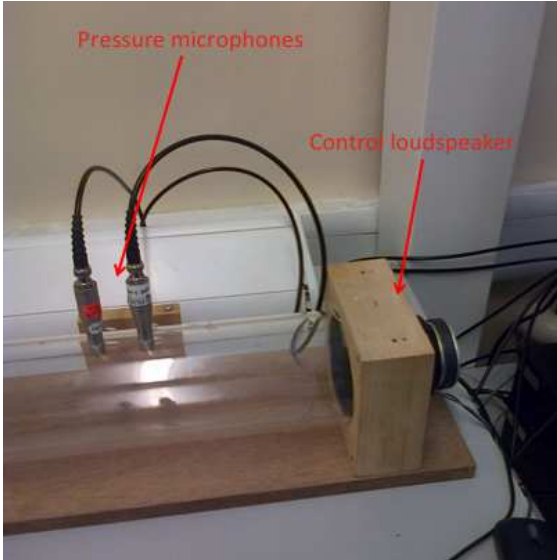
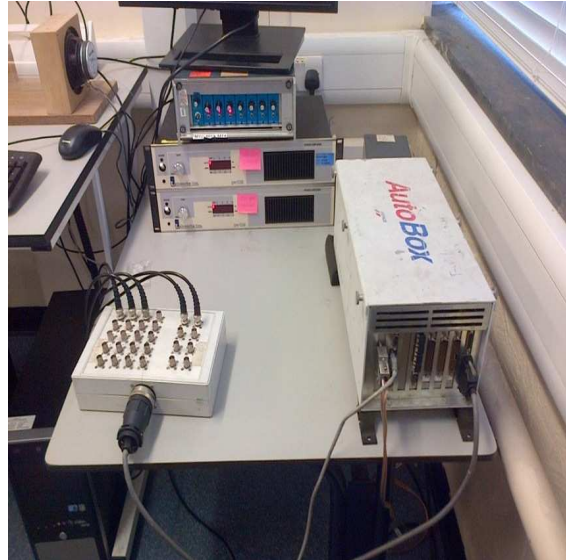


Figure 2: Illustration of the experimental acoustic duct of length  $L = 2.05 [m]$  and diameter  $d = 0.099 [m]$ . A Disturbance source at one end of the duct (D) and control source at the other end (C). Two pressure microphones are placed near the control source at distance  $\Delta x_1 = 0.0428 [m]$  from each other and  $\Delta x_2 = 0.2 [m]$  from the control loudspeaker. Microphone 1 is at distance  $x_1 = L - \Delta x_1 - \Delta x_2 = 1.8112 [m]$  and Microphone 2 at distance  $x_2 = x_1 + \Delta x_1 = 1.854 [m]$ . The Accelerometer is connected on the cone of the control loudspeaker (labelled with C).



(a)



(b)

Figure 3: (a) Control loudspeaker with embedded accelerometer and two pressure microphones. (b) dSPACE PPC Controller Board, Power Amplifiers and Pre-amplifiers required to implement the proposed control strategy.

### III Calibration and Separation technique

Before any measurements are taken, it is necessary to calibrate (match) the microphones. The method of matching the microphones can be found in ISO 10534-2 standard [9]. The result of this calibration procedure is to have identical signals from both microphones over a large frequency range. The procedure designed to calibrate the microphones requires a random signal to be injected through the disturbance speaker and the data from both microphones collected. Once this step has been done, the microphones are repositioned in each other's location (swapped) for an additional measurement of random white noise. From the two measurements a filter that will compensate for phase and magnitude differences of the two microphones is derived. With the ad-

dition of this filter the microphones are now matched. When applying the filter, the signal recorded by both microphones will be nearly identical. Finally, because the driving signal was random white noise (covering the full frequency range needed to perform experiments) the matching of the microphones is assured over this frequency range and thus control can be safely applied on the full range of frequencies.

Because the environment will always change (air temperature, humidity etc.) the calibration of the microphones should be performed every time experiments are carried out. Furthermore, small variations of the amplifier gains due to temperature variations can also affect the matching.

The signal retrieved from the two microphones is the superposition of two acoustic pressure waves, the incident  $p_i$  and the reflecting  $p_r$ . Due to wave periodicity the two components can be separated using signals from the two microphones that are spaced with known distance  $\Delta x_1$  from each other, as shown in figure 2. In the time domain, the total pressure wave (incident and reflecting) has the following mathematical form [10]:

$$p_{tot}(x, t) = p_i(x, t) + p_r(x, t) \quad (1)$$

With the illustrated experimental set-up, the microphones pick up the following pressure signals [10], respectively:

$$mic_1 = p_i(x_1, t) + p_r(x_1, t) \quad (2)$$

$$mic_2 = p_i(x_1 + \Delta x_1, t) + p_r(x_1 + \Delta x_1, t) = p_i(x_1, t + \tau) + p_r(x_1, t - \tau) \quad (3)$$

Where  $\tau = \Delta x_1/c$  [s] and is the time required for the acoustic wave to travel the predetermined distance  $\Delta x_1$  between the two microphones (0.0428 [m] , figure 2) and  $c$  is the speed of sound in air (for the experimental case studied a value of 343.3 [m/s] is assumed). If a time delay equal to  $\tau$  is applied to the signal from microphone 2 and the signal from microphone 1 is subtracted then the following result is achieved [10]:

$$mic_{2\tau} = p_i(x_1, t) + p_r(x_1, t - 2\tau) \quad (4)$$

$$P_{ref} = mic_{2\tau} - mic_1 = p_r(x_1, t) + p_r(x_1, t - 2\tau) \quad (5)$$

Therefore, as required, the acoustic pressure signal derived in equation (5) contains only components of the reflected wave. Due to the distance of the microphones, (fig. 1), in order to successfully separate the standing wave into incident and reflecting the appropriate time delay required will be  $\tau = \Delta x_1/c = 0.0428/343.3 = 0.000125$  [s] hence a sampling rate of 8 kHz is required. From Shanon's criterion the un-modelled states of  $P_{ref}$  will be above 4 kHz. For sound waves with frequencies above 4 kHz the wavelength will be smaller than  $\Delta x_1$  (distance of microphones). This implies that multiple waves will be present in the gap between the two microphones when considering frequencies greater than 4 kHz (this is equivalent to a spatial Nyquist cut-off frequency).

## IV $H_2$ feedback control

In this section a brief explanation of the control design chosen to minimise the undesired reflecting sound is presented. An  $H_2$  controller design will be considered; therefore

a Linear Fractional Transformation (LFT) expression of the mathematical model is required. The architecture utilised is illustrated in figure 4. The process is represented as a two-input and two-output system that is labelled as  $P$  and has a feedback controller  $K$  that maps the measurable signal  $w_{loud}$  to the manipulated variable  $E_{con}$ . Specifically the two inputs are the voltage of the disturbance loudspeaker  $E_{dis}$  and the voltage of the control loudspeaker  $E_{con}$ , the two outputs are the signal generated by the two microphones when using equation (5) ( $P_{ref}$ ) which is to be minimised and  $w_{loud}$  the signal measured by the accelerometer embedded on the control loudspeaker's cone. The matrix representation of the open loop system is therefore:

$$\begin{bmatrix} P_{ref} \\ w_{loud} \end{bmatrix} = \begin{bmatrix} P_{11} & P_{12} \\ P_{21} & P_{22} \end{bmatrix} \begin{bmatrix} E_{dis} \\ E_{con} \end{bmatrix} \quad (6)$$

For the implementation of the  $H_2$  design all four transfer functions  $P_{ij}$  ( $i = 1, 2$  and  $j = 1, 2$ ) have to be identified. The identification procedure of the plant's transfer functions is carried out by fitting filters to experimentally retrieved data from the apparatus. Specifically the fitting is done based on the `invfreqz(.)` function found in Matlab. This function implements Levi's complex curve fitting algorithm [11].

The next step is to formulate the  $H_2$  problem, based on equation (6) with the LFT description used for the overall system (figure 4).

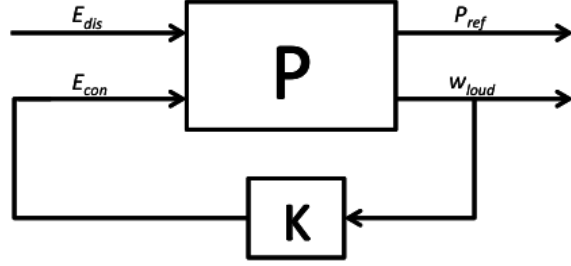


Figure 4: Block diagram of LFT description

The goal is to minimise the performance measurement, which for the case considered here is the reflected sound wave in the duct ( $P_{ref}$ ). In particular the controller is to be designed to minimise the  $H_2$  norm of the closed loop transfer function between the disturbance input ( $E_{dis}$ ) and the performance output ( $P_{ref}$ ). For reasons of consistency with the control literature a discrete state space representation of the system is adopted. Specifically,  $x(k) \in \mathbb{R}^n$  is the state vector,  $d(k)$  is the disturbance input (disturbance voltage  $E_{dis}$ ),  $z(k)$  is the performance or error output (reflecting sound wave  $P_{ref}$ ) and  $y(k)$  is the measurement output (acceleration of loudspeaker cone  $w_{loud}$ ) [12]:

$$\left. \begin{aligned} x(k+1) &= Ax(k) + B_1d(k) + B_2u(k) \\ z(k) &= C_1x(k) + D_{11}d(k) + D_{12}u(k) \\ y(k) &= C_2x(k) + D_{21}d(k) + D_{22}u(k) \end{aligned} \right\} \quad (7)$$

The equivalent compact matrix representation is given by:

$$P = \left[ \begin{array}{c|cc} A & B_1 & B_2 \\ \hline C_1 & D_{11} & D_{12} \\ C_2 & D_{21} & D_{22} \end{array} \right] \quad (8)$$

Let  $z = F_l(P, K)$  where  $F_l(P, K) = P_{11} + P_{12}K(I - P_{22}K)^{-1}P_{21}$ .

The design of the optimal feedback controller is based on the popular two Riccati function method [13]. In order to generate the controller the general  $H_2$  algorithm requires the following assumptions to be valid [12]:

1.  $(A, B_2, C_2)$  is stabilizable and detectable.
2.  $D_{12}$  and  $D_{21}$  have full rank.
3.  $\begin{bmatrix} A - j\omega I & B_2 \\ C_1 & D_{21} \end{bmatrix}$  has full column rank for  $\omega$ .
4.  $\begin{bmatrix} A - j\omega I & B_1 \\ C_2 & D_{21} \end{bmatrix}$  has full column rank for  $\omega$ .
5.  $D_{11}$  and  $D_{22}$  are zero.
6.  $D_{12} = \begin{bmatrix} 0 \\ I \end{bmatrix}$  and  $D_{21} = \begin{bmatrix} 0 & I \end{bmatrix}$ .
7.  $D_{12}^T C_1 = 0$  and  $B_1 D_{21}^T = 0$ .
8.  $(A, B_1)$  is stabilizable and  $(A, C_1)$  is detectable.

Given the assumptions are satisfied, a stabilising controller  $K_{opt}(j\omega)$  exists if and only if:

1.  $X_1 \geq 0$  is a solution to the algebraic Riccati equation:

$$A^T X_1 + X_1 A + C_1^T C_1 + X_1 (-B_2 B_2^T) X_1 = 0$$

2.  $Y_1 \geq 0$  is a solution to the algebraic Riccati equation:

$$AY_1 + Y_1A^T + B_1B_1^T + Y_1(-C_1^TC_1)Y_1 = 0$$

And in conclusion, the optimal controller is then given by the following formula:

$$K_{opt}(j\omega) = \left[ \begin{array}{c|c} \hat{A}_2 & -L_2 \\ \hline F_2 & 0 \end{array} \right] \quad (9)$$

Where  $\hat{A}_2 = A + B_2F_2 + L_2C_2$ ,  $L_2 = -Y_1C_2^T$  and  $F_2 = -B_2^TX_1$ .

It must be added, that in the case where assumptions 5,6 and 7 are not met, an appropriate transformation of the state space problem is possible and will allow the designer to form a optimal controller [14]. The described methodology would be adequate to develop an optimal feedback controller but as mentioned in the previous section a sampling rate of 8 kHz is required which in turn requires a high order discrete FIR filter (greater than 1000) in order to model the plant dynamics accurately across a broad band of frequencies. The high order of the model in combination with the sampling rate initially prohibits the design of a practical broadband feedback controller. To overcome this problem an FIR model of significantly smaller order is fitted to the plants dynamics to cover the frequency bandwidth of specific interest and this model will be used to derive the feedback controller. The desired bandwidth chosen to operate the controller is from 0-250 Hz. Two reasons led to such a choice, firstly the frequency band is located at relatively low frequencies where ANC is proven to provide significantly better performance compared to traditional passive means and secondly the range of such a band would include a dominant acoustic resonance at 186 Hz. Having acquired a controller for the reduced order plant model with lower frequency resolution the next step is to transform this to operate with a sample rate of 8 kHz to enable ready application to

the experimental rig.

In order to evaluate the level of performance of the  $H_2$  feedback design it is appropriate to compare the design with a well established control design. Therefore, the FXLMS method is chosen and implemented on the apparatus.

## V FxLMS Control Design

Over the past few decades active sound control has become a realisable and efficient control concept many control algorithms have been developed. One of the most well known of which is, ‘Filtered- x’ Least Mean Squares (FxLMS), a full account of which is located in “Adaptive Signal Processing” [15]. The algorithm carries out a gradient descent adaptation rule, Least Mean Square (LMS), for a filtered version of the reference signal. It is important to emphasise the use of the filtered reference signal rather than feeding the raw error signal to the adaptation rule and by doing so, possible instability is avoided.

The popularity of this algorithm centres on its ease of implementation and robustness, i.e. convergence can be achieved with up to  $90^\circ$  phase error in the forward path estimate [16]. However the FxLMS algorithm is prone to long convergence times, especially in random noise disturbance, due to the small value of alpha (the convergence coefficient). If the alpha is increased to too high a value, instability in the system can rapidly result.

To develop the FxLMS algorithm it is prudent to begin with the standard LMS algorithm from which it originated. Figure 5 shows an active control system with a controller based on the LMS algorithm. The FIR filter output,  $y(n)$ , is expressed by

the vector inner product (for each sample instant  $n$ ):

$$y(n) = w^T(n)x(n) \quad (10)$$

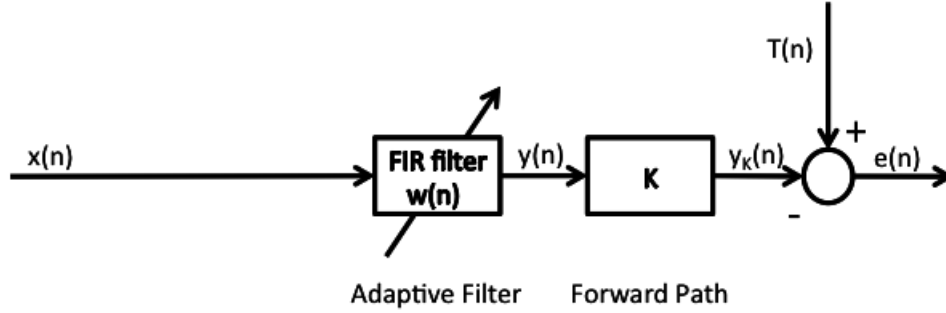


Figure 5: Block diagram of feedforward LMS algorithm.

Where  $x(n)$  is the input signal vector that is fed to the adaptive filter and is expressed as:

$$x(n) = [x(n), x(n-1), \dots, x(n-M+1)]^T \quad (11)$$

Furthermore  $w(n)$ , is the vector of filter coefficients to be found:

$$w(n) = [w_0(n), w_1(n), \dots, w_{M-1}(n)]^T \quad (12)$$

In control applications, the estimation error  $e(n)$  is defined by the difference between the desired signal (desired response)  $d(n)$  and the output signal from the forward path or plant under control  $y_C(n)$ :

$$e(n) = d(n) - y_C(n) \quad (13)$$

If it is assumed that the the transfer function of the control path can be represented by an  $I - th$  order FIR filter the following mathematical description is valid:

$$h_C(n) = \begin{cases} c_n & \text{when } n \in \{0, \dots, I - 1\} \\ 0 & \text{otherwise} \end{cases} \quad (14)$$

With this the error can be represented by:

$$e(n) = d(n) - \sum_{i=0}^{I-1} c_i \sum_{m=0}^{M-1} w_m(n-i)x(n-i-m) \quad (15)$$

The Wiener (Mean Square Error) solution of the coefficient vector is obtained by minimising the quadratic function [16, 15]:

$$J_f(n) = E[e^2(n)] \quad (16)$$

And this can be carried out by using the gradient vector for the mean square error  $J_f(n)$ :

$$\nabla_{w(n)} J_f(n) = 2E[e(n)\nabla_{w(n)}e(n)] \quad (17)$$

By taking advantage of the fact that the desired signal  $d(n)$  is independent of the filter coefficients and by assuming that  $w_m(n), m \in \{0, \dots, M - 1\}$  is time invariant, the gradient vector for the estimation error can be expressed as:

$$\nabla_{w(n)}e(n) = \begin{bmatrix} -\sum_{i=0}^{I-1} c_i x(n-i) \\ -\sum_{i=0}^{I-1} c_i x(n-i-1) \\ \vdots \\ -\sum_{i=0}^{I-1} c_i x(n-i-M+1) \end{bmatrix} \quad (18)$$

By inserting equation (18) in equation (17) we obtain the following relation for the gradient vector of the mean square error:

$$\nabla_{w(n)}J_f(n) = -2E[e(n)x_C(n)] \quad (19)$$

Where  $x_C(n)$  is given by the following vector:

$$x_C(n) = \begin{bmatrix} -\sum_{i=0}^{I-1} c_i x(n-i) \\ -\sum_{i=0}^{I-1} c_i x(n-i-1) \\ \vdots \\ -\sum_{i=0}^{I-1} c_i x(n-i-M+1) \end{bmatrix} \quad (20)$$

The LMS with a gradient estimate is then given by:

$$\nabla_{w(n)}J_f^*(n) = -2e(n)x_C(n) \quad (21)$$

would solve the problem of producing an estimate via a dynamic system [16, 17]. From this it follows that the conventional LMS algorithm is likely to be unstable in control applications. The conventional LMS algorithm will in some cases also find a poor solution when it converges [18, 16, 17]. This can be explained by the fact that the

LMS algorithm uses a gradient estimate  $x(n)e(n)$  which is not correct in the mean [18].

A compensated algorithm is obtained by filtering the reference signal to the coefficient adjustment algorithm using a model of the forward path. The Active control system with a controller based on the FxLMS algorithm is illustrated in 6 [19].

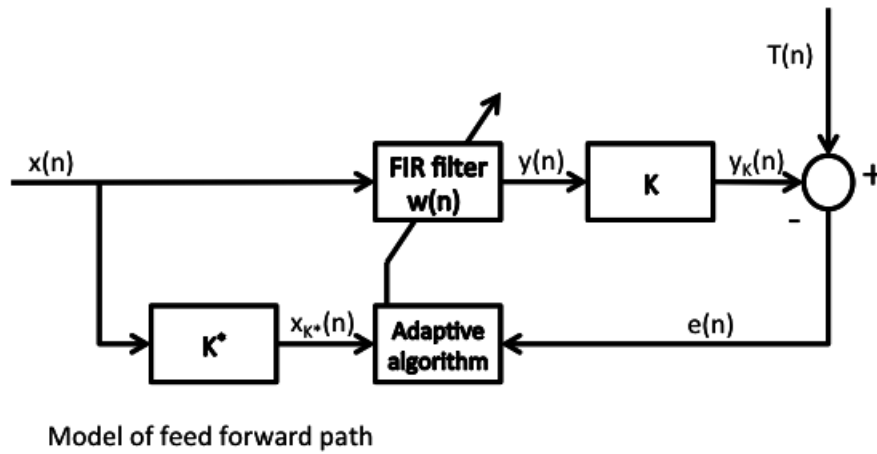


Figure 6: Block diagram of a plant with an active controller tuned with the FxLMS algorithm

The FxLMS algorithm is given by the following equations:

$$y(n) = w^T(n)x(n) \quad (22)$$

$$e(n) = d(n) - y_C(n) \quad (23)$$

$$x_{C^*}(n) = \begin{bmatrix} -\sum_{i=0}^{I-1} c_i^* x(n-i) \\ -\sum_{i=0}^{I-1} c_i^* x(n-i-1) \\ \vdots \\ -\sum_{i=0}^{I-1} c_i^* x(n-i-M+1) \end{bmatrix} \quad (24)$$

And so the update of the weights in the adaptive filter is:

$$w(n+1) = w(n) + \mu x_{C^*}(n)e(n) \quad (25)$$

Here  $\mu$  is the convergence coefficient and  $c_i^*$  are the coefficients of an estimated FIR filter model of the forward path:

$$h_{C^*}(n) = \begin{cases} c_n^* & \text{when } n \in \{0, \dots, I-1\} \\ 0 & \text{otherwise} \end{cases} \quad (26)$$

It is in practice customary to use an estimate of the impulse response for the forward path. As a result, the reference signal  $x_C^*(n)$  will be an approximation, and differences between the estimate of the forward path and the true forward path influence both the stability properties and the convergence rate of the algorithm [18, 16, 17]. However, the algorithm is robust to errors in the estimate of the forward path [18, 16, 17]. The model used should introduce a time delay corresponding to the forward paths at the dominating frequencies [18, 17]. In the case of narrow-band reference signals to the algorithm the algorithm will converge with phase errors in the estimate of the forward path with up to  $90^\circ$ , provided that the convergence coefficient  $\mu$  is sufficiently small [16, 20]. Furthermore, phase errors in the estimate of the forward path smaller

than  $45^\circ$  will have only a minor influence on the algorithm convergence rate [20].

In order to ensure that the action of the FxLMS algorithm is stable the maximum value for the convergence coefficient  $\mu$  should be given approximately by [21]:

$$\mu_{max} \approx \frac{2}{E[x^2 C^*(n)](M + \delta)} \quad (27)$$

where  $\delta$  is the overall delay in the forward path (in samples  $n$ ).

The block diagram utilised for the purpose of tuning the adaptive controller is viewed in figure 7.

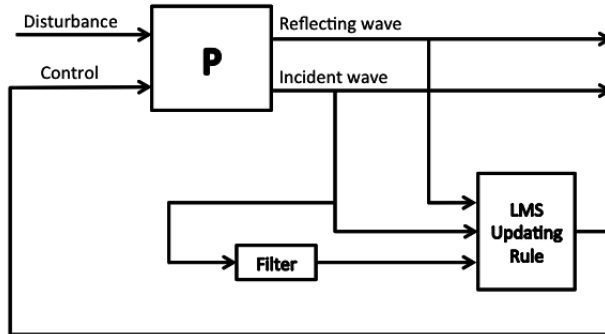


Figure 7: Block diagram for implementing FxLMS design.  $P$  is the *MIMO* plant's dynamics. The block with label filter is a transfer function that replicates the path between control to reflecting wave. Finally the updating rule block is formulated based on the theory developed in the previous chapter.

## VI Results and analysis

As mentioned in the previous section, models of the control and disturbance paths are required in order to derive the  $H_2$  controller. The frequency response of the high order FIR models of the plant together with experimentally derived data are illustrated in

figure 8. In more detail, figure 8 shows the disturbance and control paths of the acoustic duct set-up previously described in equation (6). From figure 8 it is clear that the high order FIR model of the plant provides an ideal fit and includes with high precision the dynamics of the pulse tube and loudspeakers. Furthermore, due to the high precision of the control path model it is possible to inspect the stability and robustness of a control design before it is applied directly on the pulse tube preventing any potential damage to the equipment. **It must be emphasised that for the needs of this experiment, a random white noise signal was injected to the plant via the disturbance path (disturbance loudspeaker). The choice of white noise was done in order to guaranty the excitation of all the acoustic resonances found in the apparatus.**

However as noted above, due to the high order of the model used to describe the plants dynamics, a stable and implementable feedback controller requires a reduced order plant with good accuracy across a smaller frequency range. The frequency response of the reduced order model is illustrated in figure 9. The reduced order model is also highly accurate across the targeted range. **The sample rate of the reduced order plant has to remain at 8 kHz. This is due to the distance  $\Delta x_1$  between the two microphones and the separation method implemented to acquire the reflecting sound wave. The predictions of the reduced order model beyond the range of interest will be poor as the dynamics of the plant are not consider during the fitting procedure.**

The performance of the  $H_2$  control design is demonstrated with a experimental response of the plant, figure 10. Because the controller is designed based on a reduced order model for a frequency band between 0-250 Hz the beneficial effect of the  $H_2$  feedback controller is most clearly observed with a significant 10 dB reduction at the dominant acoustic resonance located at 186 Hz. Since this is the only significant

resonance within the design bandwidth the higher order modes remain unaffected. Depending on the application and disturbance source, the higher order modes could be included by systematically extending the order of the model and controller.

In order to evaluate the level of performance of the FxLMS controller applied on the apparatus, the magnitude of the reflecting wave's power spectral density is illustrated in figure 11. By selecting an order of 256 for the adaptive controller, the design reduces the reflecting sound wave for a bandwidth of 100 – 800 Hz. The high order of the controller allows a significant reduction of the reflecting sound wave. Specifically in figure 11, a minimum reduction of  $15dB$  and maximum of  $30dB$  can be viewed after the first acoustic resonance ( $185Hz$ ).

With regards to performance it can be viewed clearly that the FxLMS controller is able to reduce the undesired reflecting sound wave more than the  $H_2$  local controller. Furthermore the adaptive controller is able to apply control to a larger bandwidth compared to the  $H_2$  feedback controller. The reason the  $H_2$  controller has a smaller bandwidth is because the low order models designed to describe the plant's dynamics up to 250 Hz. However, it must be emphasised that the FxLMS algorithm implemented on the rig considers perfect conditions; meaning that the random signal that is sent to the disturbance speaker is also used as the reference signal for the design of the feedforward FIR filter. In practice the performance would not be so good as one would have to use a microphone signal that is correlated with the disturbance signal. This would lead to the problem of feedback from the secondary source to the reference signal and would require additional compensation. Such a perfect FxLMS performance is unlikely to be achievable in any practical scenario. Furthermore, in order to achieve the good performance of the adaptive controller a tedious design procedure that required

a number of trial tests on the test rig it's self in order to guarantee stability had to be conducted. In terms of implementation complexity, the  $H_2$  control design is far more superior. Specifically, the FxLMS controller requires:

- An up to date feedforward filter of the control path.
- Experimental validation of the convergence coefficient ( $\alpha$ ).
- Experimental validation of the optimal order of the adaptive control.
- The stability of the design can only be addressed online.
- Real time measurements of the remote variables (incident and reflecting sound wave).

In order to appreciate the benefits when selecting the  $H_2$  design, a summary of them is listed bellow:

- To run the controller in realtime, the  $H_2$  design requires for implementation only a local signal from the accelerometer embedded on the control loudspeaker, whereas the adaptive controller requires the signal from a pair of high precision pressure microphones that results in a considerable increase of cost and implementation complexity. The  $H_2$  requires the error signal only during the control design.
- The stability analysis of the  $H_2$  design is much simpler to carry out in comparison to the FxLMS approach and can be evaluated offline.
- The  $H_2$  controller is a fully automated design and does not require any fine tuning of parameters such as the convergence rate (FxLMS).

In conclusion, the feedback design is a much more cost and resource efficient approach in comparison to the adaptive controller. This design option is more favourable when global measurements (microphones) are not feasible for control implementation and has great potential in producing a practically viable and low cost distributed ANC system using easily accessible local measurements.

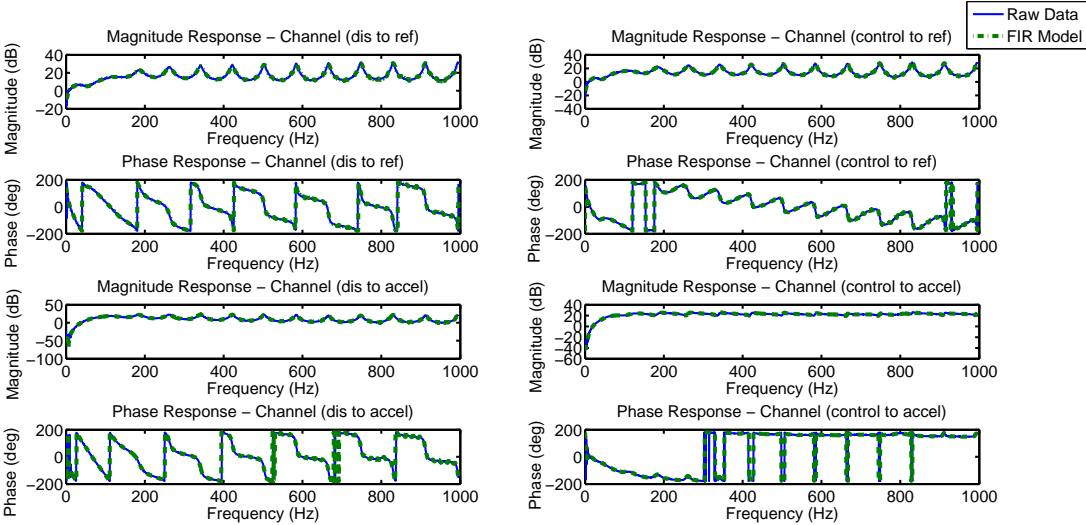


Figure 8: Bode plot of the raw experimental data for the disturbance and control paths (solid line) Bode plot of the high order FIR filter fitted to the experimental data (dashed line).

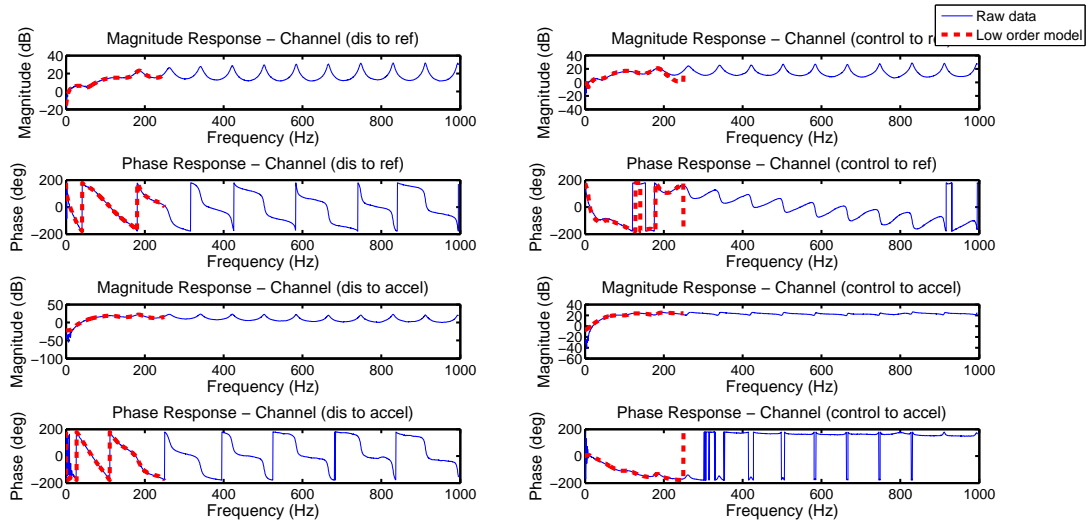


Figure 9: Bode plot of the raw experimental data for the disturbance and control paths (solid line) and Bode plot of the reduced order model fitted to the experimental data (dashed line).

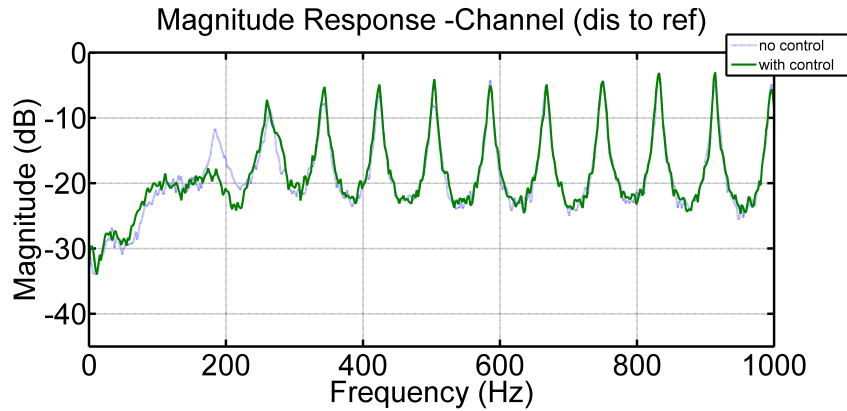


Figure 10: Magnitude of the power spectral density of the reflecting sound wave without and with local  $H_2$  feedback control for experimental data (dashed line, solid line).

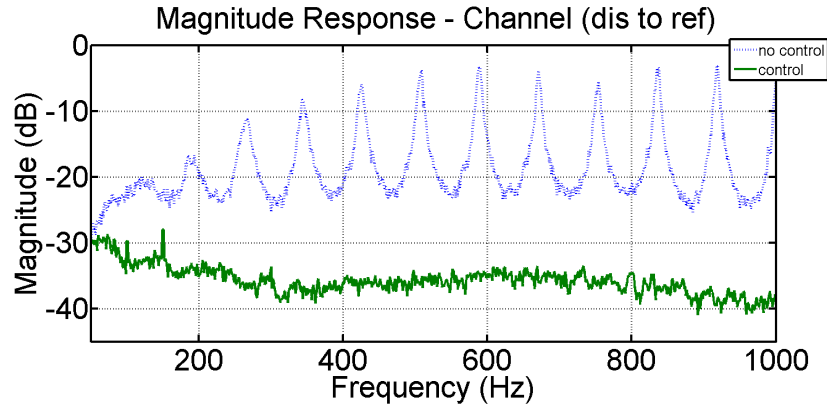


Figure 11: Magnitude of the power spectral density of the reflecting sound wave without control and with FxLMS feedforward control for experimental response (dashed line, solid line)

## VII Conclusions

In this paper a systematic approach to the design of an ANC system was developed in order to achieve reduction of the reflected sound waves in an experimental one-dimensional acoustic duct problem. The method makes use of a robust and near-optimal  $H_2$  generalised feedback controller and has been shown experimentally to be capable of a significant reduction in the undesired reflected sound waves within a design frequency bandwidth. In contrast to classical ANC approaches the suggested feedback control procedure is a locally based collocated design. The approach utilises only a local measurement of the acceleration of the boundary-reflecting surface (in the experimental case considered here, the control loudspeaker's cone) in order to produce the control signal and does not therefore during implementation require any remote measurements, such as microphones to generate the control command. In practice, this design reduces the physical size and cost of the control system and moreover reduces the complexity

of the compensator together with the associated computational burden.

## Acknowledgement

The author's would like to acknowledge support from EPSRC and the Onassis foundation during the course of this work.

## References

- [1] S.M. Kuo and D. Morgan, *Active noise control systems: algorithms and DSP implementations*, (John Wiley & Sons, Inc. New York, NY, USA, 1995) pp. 17–101.
- [2] S.M. Kuo and D.R. Morgan, "Active noise control: a tutorial review, "Proceedings of the IEEE. **87(6)**, 943–973(1999).
- [3] X. Yu and H. Zhu and R. Rajamani and K.A. Stelson, K. A., "Acoustic transmission control using active panels: an experimental study of its limitations and possibilities, "Smart Materials and Structures. **16(6)**, 2006(2007).
- [4] H. Zhu and R. Rajamani and K.A Stelson, "Active control of acoustic reflection, absorption, and transmission using thin panel speakers, "The Journal of the Acoustical Society of America. **113**, 852(2003).
- [5] Y. Lee and P. Gardonio and S.J. Elliott, "Volume velocity vibration control of a smart panel using a uniform force actuator and an accelerometer array, "Smart materials and structures. **11(6)**, 863(2002).

- [6] J. S. Vipperman and R. L. Clark, "Multivariable feedback active structural acoustic control using adaptive piezoelectric sensor/actuators," *The Journal of the Acoustical Society of America*. **105(1)**, 219–225(1999).
- [7] M. R. Bai and H. H. Lin, "Comparison of active noise control structures in the presence of acoustical feedback by using the H-infinity synthesis technique," *Journal of Sound and Vibration*. **206(4)**, 453–471(1997).
- [8] H. Lissek and R. Boulandet and R. Fleury, R., "Electroacoustic absorbers: bridging the gap between shunt loudspeakers and active sound absorption," *The Journal of the Acoustical Society of America*. **129**, 2968(2011).
- [9] ISO 10354-2: "Acoustics - Determination of sound absorption coefficient and impedance in impedance tubes - Part 2: transfer-function method, (1996).
- [10] D. Guicking, "Recent advances in active noise control," *Recent Developments in Air-and Structure-Borne Sound and Vibration*. **1**, 313–320(1992).
- [11] E. C. Levy, "Complex-Curve Fitting," *IRE Transactions on Automatic Control*. **4**, 37–44(1959).
- [12] S. Skogestad and I. Postlethwaite, *Multivariable feedback control: analysis and design, volume 2* (Wiley, England, 1997), pp. 362–365.
- [13] J.C. Doyle and K. Glover and P.P. Khargonekar and B.A. Francis, "State-space solutions to standard H2 and H-infinity control problems," *Automatic Control, IEEE Transactions on*. **34(8)**, 831–847(1989).

- [14] M. Green and D.J.N. Limebeer, *Linear robust control* (Dover Publications, Inc., Mineola, New York, 2012), pp. 131–178.
- [15] B. Widrow and S.D. Stearns, *Adaptive signal processing* (Englewood Cliffs, NJ, Prentice-Hall, Inc., 1985), chapter 3.
- [16] P.A. Nelson and S.J. Elliott and J.E.F Williams, *Active control of sound* (Academic Press Inc, London, 1993), pp. 161–200.
- [17] D.R. Morgan, D. R., “An analysis of multiple correlation cancellation loops with a filter in the auxiliary path, ”Acoustics, Speech and Signal Processing, IEEE Transactions on. **28(4)**, 454–467(1980).
- [18] S.J. Elliott and I. Stothers and P.A. Nelson, “A multiple error LMS algorithm and its application to the active control of sound and vibration, ”Acoustics, Speech and Signal Processing, IEEE Transactions on. **35(10)**, 1423–1434(1987).
- [19] L. Hakansson, “The filtered-X LMS algorithm, ”University of Karlskrona/Ronneby, 1–4 (2004).
- [20] C.C. Boucher and S.J. Elliott and P.A. Nelson, “Effect of errors in the plant model on the performance of algorithms for adaptive feedforward control,” IEE Proceedings F (Radar and Signal Processing). **138(4)**, 313–319 (1991).
- [21] S.J. Elliott and P.A. Nelson, “Multiple-point equalization in a room using adaptive digital filters, ”Journal of the Audio Engineering Society. **37(11)**, 899–907(1989).

# List of figure captions

- Figure1 Picture of the experimental acoustic tube consisting of the disturbance source (near end), control source (far end) and the three sensors (two microphones and the accelerometer).
- Figure2 Illustration of the experimental acoustic duct of length  $L = 2.05 [m]$  and diameter  $d = 0.099 [m]$ . A Disturbance source at one end of the duct (D) and control source at the other end (C). Two pressure microphones are placed near the control source at distance  $\Delta x_1 = 0.0428 [m]$  from each other and  $\Delta x_2 = 0.2 [m]$  from the control loudspeaker. Microphone 1 is at distance  $x_1 = L - \Delta x_1 - \Delta x_2 = 1.8112 [m]$  and Microphone 2 at distance  $x_2 = x_1 + \Delta x_1 = 1.854 [m]$ . The Accelerometer is connected on the cone of the control loudspeaker (labelled with C).
- Figure3 (a) Control loudspeaker with embedded accelerometer and two pressure microphones. (b) dSPACE PPC Controller Board, Power Amplifiers and Pre-amplifiers required to implement the proposed control strategy.
- Figure4 Block diagram of LFT description.
- Figure5 Block diagram of feedforward LMS algorithm.
- Figure6 Block diagram of a plant with an active controller tuned with the FxLMS algorithm.
- Figure7 Block diagram for implementing FxLMS design.  $P$  is the *MIMO* plant's dynamics. The block with label filter is a transfer function that replicates

the path between control to reflecting wave. Finally the updating rule block is formulated based on the theory developed in the previous chapter.

Figure8 Bode plot of the raw experimental data for the disturbance and control paths (solid line) and Bode plot of the high order FIR filter fitted to the experimental data (dashed line).

Figure9 Bode plot of the raw experimental data for the disturbance and control paths (solid line) and Bode plot of the reduced order FIR filter fitted to the experimental data (dashed line).

Figure10 Magnitude of the power spectral density of the reflecting sound wave without and with local  $H_2$  feedback control for experimental data (dashed line, solid line).

Figure11 Magnitude of the power spectral density of the reflecting sound wave without control and with FxLMS feedforward control for experimental response (dashed line, solid line).

## List of notations

$c$	Speed of sound in air
$d$	Diameter of acoustic duct cross section
$d(n)$	Desired signal (FxLMS algorithm)
$e(n)$	Estimation error (FxLMS algorithm)

$j$	Imaginary number
$h_C(n)$	FIR filter describing the control path
$mic_1$	Signal picked from microphone 1
$mic_2$	Signal picked from microphone 2
$mic_{2\tau}$	Signal picked from microphone 2 with delay
$p_i$	Incident acoustic wave
$p_r$	Reflecting acoustic wave
$w(n)$	FIR feedforward filter coefficients (FxLMS algorithm)
$w_{loud}$	Signal from accelerometer
$y(n)$	Output from feedforward FIR filter (FxLMS algorithm)
$y_C(n)$	Output signal from forward path (FxLMS algorithm)
$x(n)$	Input Signal (FxLMS algorithm)
$\mu$	Convergence coefficient (FxLMS algorithm)
$\tau$	Time required for sound to travel $\Delta x_1$
ANC	Active noise control
ASAC	Active Structural Acoustic Control
$E_{con}$	Voltage of control loudspeaker

$E_{dis}$	Voltage of disturbance loudspeaker
FIR	Finite Impulse Response Filter
FxLMS	Filtered -x Least Mean Square
GCC	General Control Configuration
$I$	Identity matrix
$J_f(n)$	Mean square error (FxLMS algorithm)
$K$	Feedback Controller
$K_{opt}$	Optimal feedback controller
$L$	Length of acoustic duct
LFT	Linear Fractional Transformation
$P$	Compact matrix representation of discrete state space model of a plant
$P_{tot}$	Total acoustic pressure wave
$P_{ref}$	Expression of reflected sound wave
$\Delta x_1$	Distance of microphone 1 from control loudspeaker
$\Delta x_2$	Distance of microphone 2 from control loudspeaker